



Vibration analysis of functionally graded plates with porosity composed of a mixture of Aluminum (Al) and Alumina (Al_2O_3) embedded in an elastic medium

Saidi Hayat, Sahla Meriem

Civil Engineering Department, Faculty of Technology, University of Sidi Bel Abbes, Laboratory of Materials and Hydrology (LMH), Algeria.

hayatsaidi2019@yahoo.fr, meriemsahla@gmail.com

ABSTRACT In this scientific work, a new shear deformation theory for free vibration analysis of simply supported rectangular functionally graded plate embedded in an elastic medium is presented.

Due to technical problems during the fabrication, porosities can be created inside FGM plate which may lead to reduction in strength of materials. In this investigation the FGM plate are assumed to have a new distribution of porosities according to the thickness of the plate. The elastic medium is modeled as Winkler-Pasternak two parameter models to express the interaction between the FGM plate and elastic foundation. The four unknown shear deformation theory is employed to deduce the equations of motion. The Hamilton's principle is used to derive the governing equations of motion. The accuracy of this theory is verified by compared the developed results with those obtained using others plate theory. Some examples are performed to demonstrate the effect of changing gradient material, elastic parameters, porosity index, and length to thickness ratios on the fundamental frequency of functionally graded plate.

KEYWORDS. Shear deformation theory; Vibration; Functionally graded plate; Porosity; Frequency.



Citation: Saidi, H., Sahla, M., Vibration analysis of functionally graded plates with porosity composed of a mixture of Aluminum (Al) and Alumina (Al_2O_3) embedded in an elastic medium, *Frattura ed Integrità Strutturale*, 50 (2019) 286-299.

Received: 20.07.2019

Accepted: 19.08.2019

Published: 01.10.2019

Copyright: © 2019 This is an open access article under the terms of the CC-BY 4.0, which permits unrestricted use, distribution, and reproduction in any medium, provided the original author and source are credited.

INTRODUCTION

Functionally graded materials (FGMs) are a type of heterogeneous composite materials that exhibits a continuous variation of mechanical properties from one point to another. The concept of functionally graded material was first considered in Japan in 1984 during a space plane project.

Such kind material is produced by mixing two or more materials by a graded distribution of the volume fractions of the constituents [1], the FGM is thus suitable for diverse applications, such as thermal coatings of barrier for ceramic engines, electrical devices, energy transformation, biomedical engineering, optics, etc [2-11].

However, in FGM fabrication, micro voids or porosities can occur within the materials during the process of sintering. This is because of the large difference in solidification temperatures between material constituents [12].

Wattanasakulpong [13], also gave the discussion on porosities happening inside FGM samples fabricated by a multi-step sequential infiltration technique. Therefore, it is important to take into account the porosity effect when designing FGM structures subjected to dynamic loadings [14]. Currently, many functionally graded (FG) plate structures which have been employed for engineering fields led to the development of various plate models to study the static, buckling and vibration responses of FG structures [15-19]. The classical plate theory (CPT) is based on the supposition that straight lines which are normal to the neutral surface before deformation remain straight and normal to the neutral surface after deformation. Since the transverse shear deformation is neglected [20-23], it cannot be suitable for the investigating of moderately thick or thick plates in which transverse shear deformation effects are more important. For FG thick and moderately thick plates; the first-order shear deformation theory (FSDT) has been employed [24-27]. In such formulation, the displacements are linearly varied within the thickness and need a shear correction coefficient to correct the unrealistic distribution of the transverse shear stresses and shear strains across the thickness. To avoid the use of the shear correction coefficient, higher-order shear deformation plate theories (HSDTs) have been developed [28-40].

The purpose of this work to propose a new higher-order shears deformation theory for free vibration response of FG plates with porosity embedded in elastic medium. In this investigation the FGM plate are assumed to have a new distribution of porosity according to the thickness of the plate. The elastic medium is modeled as Winkler-Pasternak two parameter models to express the interaction between the FGM plate and elastic foundation. The four unknown shear deformation theory is employed to deduce the equations of motion from Hamilton's principle. The Hamilton's principle is used to derive the governing equations of motion. The accuracy of this theory is verified by compared the developed results with those obtained using others plate theory. Some examples are performed to demonstrate the effect of changing gradient material, elastic parameters, porosity index, and length to thickness ratios on the fundamental frequency of functionally graded plate.

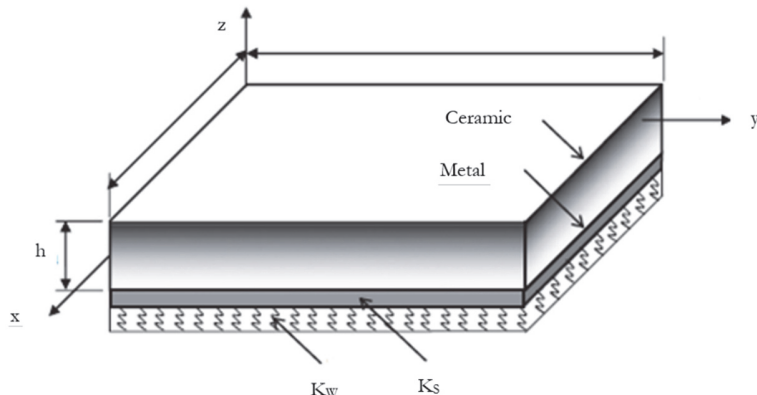


Figure 1: Schematic representation of a rectangular FG plate resting on elastic foundation.

MATHEMATICAL FORMULATION

In the current work, a FG simply supported rectangular plate with length, width and uniform thickness equal to a , b and h respectively is considered. The geometry of the plate and coordinate system are illustrated in Fig. 1. The material characteristics of FG plate are considered to vary continuously within the thickness of the plate in according to the power law distribution as follows

$$E(z) = E_m + (E_c - E_m) \left(\frac{1}{2} + \frac{z}{h} \right)^k - (E_c - E_m) (1 - e^{(-\xi/2)}) \quad (1a)$$

$$\rho(z) = \rho_m + (\rho_c - \rho_m) \left(\frac{1}{2} + \frac{z}{h} \right)^k - (E_c - E_m) (1 - e^{(-\xi/2)}) \quad (1b)$$



where the subscripts m and c denote the metallic and ceramic components, respectively; and p is the power law exponent. The value of k equal to zero indicates a fully ceramic plate, whereas infinite p represents a fully metallic plate. Since the influences of the variation of Poisson's ratio ν on the behavior of FG plates are very small [37], it is supposed to be constant for convenience.

ξ is the factor of the distribution of the porosity according to the thickness of the plate [41].

KINEMATICS AND STRAINS

In this investigation, further simplifying supposition are made to the conventional higher shear deformation theory (HSDT) so that the number of unknowns is reduced. The displacement field of the conventional HSDT is expressed by Saidi et al [40].

$$u(x, y, z, t) = u_0(x, y, t) - z \frac{\partial w_0}{\partial x} + f(z)\theta_x(x, y, t) \quad (2a)$$

$$v(x, y, z, t) = v_0(x, y, t) - z \frac{\partial w_0}{\partial y} + f(z)\theta_y(x, y, t) \quad (2b)$$

$$w(x, y, z, t) = w_0(x, y, t) \quad (2c)$$

where the shape function $f(z)$ is chosen according to Mahi et al [42]:

$$f(z) = \frac{b}{2} \tanh\left(2 \frac{z}{b}\right) - \frac{4}{3 \cosh^2(1)} \left(\frac{z^3}{b^2} \right) \quad (3)$$

Clearly, the displacement field in Eq. (2) considers only four unknowns (u_0, v_0, w_0 and ϕ). The nonzero strains associated with the displacement field in Eq. (2) are:

$$\begin{Bmatrix} \epsilon_x \\ \epsilon_y \\ \gamma_{xy} \end{Bmatrix} = \begin{Bmatrix} \epsilon_x^0 \\ \epsilon_y^0 \\ \gamma_{xy}^0 \end{Bmatrix} + z \begin{Bmatrix} k_x^b \\ k_y^b \\ k_{xy}^b \end{Bmatrix} + f(z) \begin{Bmatrix} k_x^s \\ k_y^s \\ k_{xy}^s \end{Bmatrix}, \quad \begin{Bmatrix} \gamma_{yz} \\ \gamma_{xz} \end{Bmatrix} = g(z) \begin{Bmatrix} \gamma_{yz}^0 \\ \gamma_{xz}^0 \end{Bmatrix} \quad (4)$$

where

$$\begin{Bmatrix} \epsilon_x^0 \\ \epsilon_y^0 \\ \gamma_{xy}^0 \end{Bmatrix} = \begin{Bmatrix} \frac{\partial u_0}{\partial x} \\ \frac{\partial v_0}{\partial x} \\ \frac{\partial u_0}{\partial y} + \frac{\partial v_0}{\partial x} \end{Bmatrix}, \quad \begin{Bmatrix} k_x^b \\ k_y^b \\ k_{xy}^b \end{Bmatrix} = \begin{Bmatrix} -\frac{\partial^2 w_0}{\partial x^2} \\ -\frac{\partial^2 w_0}{\partial y^2} \\ -2 \frac{\partial^2 w_0}{\partial x \partial y} \end{Bmatrix}, \quad \begin{Bmatrix} k_x^s \\ k_y^s \\ k_{xy}^s \end{Bmatrix} = \begin{Bmatrix} -\frac{\partial^2 \phi}{\partial x^2} \\ -\frac{\partial^2 \phi}{\partial y^2} \\ -2 \frac{\partial^2 \phi}{\partial x \partial y} \end{Bmatrix}, \quad \begin{Bmatrix} \gamma_{yz}^0 \\ \gamma_{xz}^0 \end{Bmatrix} = \begin{Bmatrix} \frac{\partial \phi}{\partial y} \\ \frac{\partial \phi}{\partial x} \end{Bmatrix} \quad (5a)$$

and

$$g(z) = -\frac{df(z)}{dz} \quad (5b)$$



For elastic and isotropic FGMs, the constitutive relations can be expressed as:

$$\begin{Bmatrix} \sigma_x \\ \sigma_y \\ \tau_{xy} \\ \tau_{yx} \\ \tau_{xx} \end{Bmatrix} = \begin{bmatrix} C_{11} & C_{12} & 0 & 0 & 0 \\ C_{12} & C_{22} & 0 & 0 & 0 \\ 0 & 0 & C_{66} & 0 & 0 \\ 0 & 0 & 0 & C_{44} & 0 \\ 0 & 0 & 0 & 0 & C_{55} \end{bmatrix} \begin{Bmatrix} \varepsilon_x \\ \varepsilon_y \\ \gamma_{xy} \\ \gamma_{yx} \\ \gamma_{xx} \end{Bmatrix} \quad (6)$$

where $(\sigma_x, \sigma_y, \tau_{xy}, \tau_{yx}, \tau_{xx})$ and $(\varepsilon_x, \varepsilon_y, \gamma_{xy}, \gamma_{yx}, \gamma_{xx})$ are the stress and strain components, respectively. Using the material properties defined in Eq. (1), stiffness coefficients, C_{ij} , can be written as

$$C_{11} = C_{22} = \frac{E(z)}{1-\nu^2}, \quad C_{12} = \frac{\nu E(z)}{1-\nu^2}, \quad C_{44} = C_{55} = C_{66} = \frac{E(z)}{2(1+\nu)} \quad (7)$$

EQUATION OF MOTION

Hamilton's principle is herein employed to determine the equations of motion:

$$0 = \int_0^t (\delta U + \delta V - \delta K) dt \quad (8)$$

where δU is the variation of strain energy; δV is the variation of work done; and δK is the variation of kinetic energy.

The variation of strain energy of the plate is computed by

$$\begin{aligned} \delta U &= \int_V [\sigma_x \delta \varepsilon_x + \sigma_y \delta \varepsilon_y + \tau_{xy} \delta \gamma_{xy} + \tau_{yx} \delta \gamma_{yx} + \tau_{xx} \delta \gamma_{xx}] dV \\ &= \int_A [N_x \delta \varepsilon_x^0 + N_y \delta \varepsilon_y^0 + N_{xy} \delta \gamma_{xy}^0 + M_x^b \delta k_x^b + M_y^b \delta k_y^b + M_{xy}^b \delta k_{xy}^b \\ &\quad + M_x^s \delta k_x^s + M_y^s \delta k_y^s + M_{xy}^s \delta k_{xy}^s + S_{yx}^s \delta \gamma_{yx}^s + S_{xx}^s \delta \gamma_{xx}^s] dA = 0 \end{aligned} \quad (9)$$

where A is the top surface and the stress resultants N , M , and S are defined by

$$(N_i, M_i^b, M_i^s) = \int_{-b/2}^{b/2} (1, z, f) \sigma_i dz, \quad (i = x, y, xy) \quad \text{and} \quad (S_{xx}^s, S_{yx}^s) = \int_{-b/2}^{b/2} g(\tau_{xx}, \tau_{yx}) dz \quad (10)$$

The variation of the potential energy of elastic foundation can be calculated by

$$\delta V = \int_A f_e \delta w_0 dA \quad (11)$$

where f_e is the density of reaction force of foundation.

For the Pasternak foundation model [43-53].

$$f_e = K_W w - K_{S1} \frac{\partial^2 w}{\partial x^2} - K_{S2} \frac{\partial^2 w}{\partial y^2} \quad (12)$$



where K_W is the modulus of subgrade reaction (elastic coefficient of the foundation) and K_{s1} and K_{s2} are the shear moduli of the subgrade (shear layer foundation stiffness). If foundation is homogeneous and isotropic, we will get $K_{s1} = K_{s2} = K_s$. If the shear layer foundation stiffness is neglected, Pasternak foundation becomes a Winkler foundation. The variation of kinetic energy of the plate can be expressed as:

$$\begin{aligned} \delta K &= \int_V [\dot{u}\delta\dot{u} + \dot{v}\delta\dot{v} + \dot{w}\delta\dot{w}] \rho(\tilde{z}) dV \\ &= \int_A \left\{ I_0 [\dot{u}_0\delta\dot{u}_0 + \dot{v}_0\delta\dot{v}_0 + \dot{w}_0\delta\dot{w}_0] \right. \\ &\quad - I_1 \left(\dot{u}_0 \frac{\partial\delta\dot{w}_0}{\partial x} + \frac{\partial\dot{w}_0}{\partial x} \delta\dot{u}_0 + \dot{v}_0 \frac{\partial\delta\dot{w}_0}{\partial y} + \frac{\partial\dot{w}_0}{\partial y} \delta\dot{v}_0 \right) \\ &\quad - J_1 \left(\dot{u}_0 \frac{\partial\delta\dot{\phi}}{\partial x} + \frac{\partial\dot{\phi}}{\partial x} \delta\dot{u}_0 + \dot{v}_0 \frac{\partial\delta\dot{\phi}}{\partial y} + \frac{\partial\dot{\phi}}{\partial y} \delta\dot{v}_0 \right) \\ &\quad + I_2 \left(\frac{\partial\dot{w}_0}{\partial x} \frac{\partial\delta\dot{w}_0}{\partial x} + \frac{\partial\dot{w}_0}{\partial y} \frac{\partial\delta\dot{w}_0}{\partial y} \right) + K_2 \left(\frac{\partial\dot{\phi}}{\partial x} \frac{\partial\delta\dot{\phi}}{\partial x} + \frac{\partial\dot{\phi}}{\partial y} \frac{\partial\delta\dot{\phi}}{\partial y} \right) \\ &\quad \left. + J_2 \left(\frac{\partial\dot{w}_0}{\partial x} \frac{\partial\delta\dot{\phi}}{\partial x} + \frac{\partial\dot{\phi}}{\partial x} \frac{\partial\delta\dot{w}_0}{\partial x} + \frac{\partial\dot{w}_0}{\partial y} \frac{\partial\delta\dot{\phi}}{\partial y} + \frac{\partial\dot{\phi}}{\partial y} \frac{\partial\delta\dot{w}_0}{\partial y} \right) \right\} dA \end{aligned}$$

where dot-superscript convention indicates the differentiation with respect to the time variable t ; $\rho(\tilde{z})$ is the mass density given by Eq. (1b); and (I_i, J_i, K_i) are mass inertias expressed by

$$(I_0, I_1, I_2) = \int_{-b/2}^{b/2} (1, \tilde{z}, \tilde{z}^2) \rho(\tilde{z}) d\tilde{z} \quad (14a)$$

$$(J_1, J_2, K_2) = \int_{-b/2}^{b/2} (f, \tilde{z}f, f^2) \rho(\tilde{z}) d\tilde{z} \quad (14b)$$

Substituting Eqs. (9), (11), and (13) into Eq. (8), integrating by parts, and collecting the coefficients of δu_0 , δv_0 , δw_0 and $\delta \phi$; the following equations of motion are obtained:

$$\begin{aligned} \delta u_0 : \quad & \frac{\partial N_x}{\partial x} + \frac{\partial N_{xy}}{\partial y} = I_0 \ddot{u}_0 - I_1 \frac{\partial \ddot{w}_0}{\partial x} - J_1 \frac{\partial \ddot{\phi}}{\partial x} \\ \delta v_0 : \quad & \frac{\partial N_{xy}}{\partial x} + \frac{\partial N_y}{\partial y} = I_0 \ddot{v}_0 - I_1 \frac{\partial \ddot{w}_0}{\partial y} - J_1 \frac{\partial \ddot{\phi}}{\partial y} \\ \delta w_0 : \quad & \frac{\partial^2 M_x^b}{\partial x^2} + 2 \frac{\partial^2 M_{xy}^b}{\partial x \partial y} + \frac{\partial^2 M_y^b}{\partial y^2} - f_e = I_0 \ddot{w}_0 + I_1 \left(\frac{\partial \ddot{u}_0}{\partial x} + \frac{\partial \ddot{v}_0}{\partial y} \right) - I_2 \nabla^2 \ddot{w}_0 - J_2 \nabla^2 \ddot{\phi} \\ \delta \phi : \quad & \frac{\partial^2 M_x^s}{\partial x^2} + 2 \frac{\partial^2 M_{xy}^s}{\partial x \partial y} + \frac{\partial^2 M_y^s}{\partial y^2} + \frac{\partial S_{xx}^s}{\partial x} + \frac{\partial S_{yy}^s}{\partial y} = J_1 \left(\frac{\partial \ddot{u}_0}{\partial x} + \frac{\partial \ddot{v}_0}{\partial y} \right) \\ & \quad - J_2 \nabla^2 \ddot{w}_0 - K_2 \nabla^2 \ddot{\phi} \end{aligned} \quad (15)$$

where $\nabla^2 = \partial^2 / \partial x^2 + \partial^2 / \partial y^2$ is the Laplacian operator in two-dimensional Cartesian coordinate system.



Substituting Eq. (4) into Eq. (6) and the subsequent results into Eqs. (10), the stress resultants are obtained in terms of strains as following compact form:

$$\begin{Bmatrix} N \\ M^b \\ M^s \end{Bmatrix} = \begin{bmatrix} A & B & B^s \\ B & D & D^s \\ B^s & D^s & H^s \end{bmatrix} \begin{Bmatrix} \boldsymbol{\varepsilon} \\ k^b \\ k^s \end{Bmatrix}, \quad S = A^s \boldsymbol{\gamma}, \quad (16)$$

in which

$$N = \{N_x, N_y, N_{xy}\}^t, \quad M^b = \{M_x^b, M_y^b, M_{xy}^b\}^t, \quad M^s = \{M_x^s, M_y^s, M_{xy}^s\}^t, \quad (17a)$$

$$\boldsymbol{\varepsilon} = \{\varepsilon_x^0, \varepsilon_y^0, \gamma_{xy}^0\}^t, \quad k^b = \{k_x^b, k_y^b, k_{xy}^b\}^t, \quad k^s = \{k_x^s, k_y^s, k_{xy}^s\}^t, \quad (17b)$$

$$A = \begin{bmatrix} A_{11} & A_{12} & 0 \\ A_{12} & A_{22} & 0 \\ 0 & 0 & A_{66} \end{bmatrix}, \quad B = \begin{bmatrix} B_{11} & B_{12} & 0 \\ B_{12} & B_{22} & 0 \\ 0 & 0 & B_{66} \end{bmatrix}, \quad D = \begin{bmatrix} D_{11} & D_{12} & 0 \\ D_{12} & D_{22} & 0 \\ 0 & 0 & D_{66} \end{bmatrix}, \quad (17c)$$

$$B^s = \begin{bmatrix} B_{11}^s & B_{12}^s & 0 \\ B_{12}^s & B_{22}^s & 0 \\ 0 & 0 & B_{66}^s \end{bmatrix}, \quad D^s = \begin{bmatrix} D_{11}^s & D_{12}^s & 0 \\ D_{12}^s & D_{22}^s & 0 \\ 0 & 0 & D_{66}^s \end{bmatrix}, \quad H^s = \begin{bmatrix} H_{11}^s & H_{12}^s & 0 \\ H_{12}^s & H_{22}^s & 0 \\ 0 & 0 & H_{66}^s \end{bmatrix}, \quad (17d)$$

$$S = \{S_{xx}^s, S_{yy}^s\}^t, \quad \boldsymbol{\gamma} = \{\gamma_{xx}^0, \gamma_{yy}^0\}^t, \quad A^s = \begin{bmatrix} A_{44}^s & 0 \\ 0 & A_{55}^s \end{bmatrix}, \quad (17e)$$

and stiffness components are given as:

$$\begin{Bmatrix} A_{11} & B_{11} & D_{11} & B_{11}^s & D_{11}^s & H_{11}^s \\ A_{12} & B_{12} & D_{12} & B_{12}^s & D_{12}^s & H_{12}^s \\ A_{66} & B_{66} & D_{66} & B_{66}^s & D_{66}^s & H_{66}^s \end{Bmatrix} = \int_{-b/2}^{b/2} C_{11}(1, \zeta, \zeta^2, f(\zeta), \zeta f(\zeta), f^2(\zeta)) \begin{Bmatrix} 1 \\ \nu \\ \frac{1-\nu}{2} \end{Bmatrix} d\zeta, \quad (18a)$$

$$(A_{22}, B_{22}, D_{22}, B_{22}^s, D_{22}^s, H_{22}^s) = (A_{11}, B_{11}, D_{11}, B_{11}^s, D_{11}^s, H_{11}^s), \quad (18b)$$

$$A_{44}^s = A_{55}^s = \int_{-b/2}^{b/2} C_{44} [g(\zeta)]^2 d\zeta, \quad (18c)$$

ANALYTICAL SOLUTION FOR SIMPLY-SUPPORTED FG PLATES

Based on Navier technique, the following expansions of generalized displacements are considered to automatically respect the simply supported boundary conditions:



$$\begin{Bmatrix} u_0 \\ v_0 \\ w_0 \\ \phi \end{Bmatrix} = \sum_{m=1}^{\infty} \sum_{n=1}^{\infty} \begin{Bmatrix} U_{mn} e^{i\omega t} \cos(\alpha x) \sin(\beta y) \\ V_{mn} e^{i\omega t} \sin(\alpha x) \cos(\beta y) \\ W_{mn} e^{i\omega t} \sin(\alpha x) \sin(\beta y) \\ X_{mn} e^{i\omega t} \sin(\alpha x) \sin(\beta y) \end{Bmatrix} \quad (19)$$

where $\alpha = m\pi/a$ and $\beta = n\pi/b$, ω is the frequency of free vibration of the plate, $\sqrt{i} = -1$ the imaginary unit.

Substituting Eqs. (19) into Eq. (15) and collecting the displacements and acceleration for any values of m and n , the following problem is obtained:

$$\begin{Bmatrix} S_{11} & S_{12} & S_{13} & S_{14} \\ S_{12} & S_{22} & S_{23} & S_{24} \\ S_{13} & S_{23} & S_{33} & S_{34} \\ S_{14} & S_{24} & S_{34} & S_{44} \end{Bmatrix} - \omega^2 \begin{Bmatrix} m_{11} & 0 & m_{13} & m_{14} \\ 0 & m_{22} & m_{23} & m_{24} \\ m_{13} & m_{23} & m_{33} & m_{34} \\ m_{14} & m_{24} & m_{34} & m_{44} \end{Bmatrix} \begin{Bmatrix} U_{mn} \\ V_{mn} \\ W_{mn} \\ X_{mn} \end{Bmatrix} = \begin{Bmatrix} 0 \\ 0 \\ 0 \\ 0 \end{Bmatrix} \quad (20)$$

where

$$\begin{aligned} S_{11} &= A_{11}\alpha^2 + A_{66}\beta^2, \quad S_{12} = \alpha\beta(A_{12} + A_{66}), \quad S_{13} = -\alpha(B_{11}\alpha^2 + B_{12}\beta^2 + 2B_{66}\beta^2), \quad S_{14} = -\alpha(B_{11}^s\alpha^2 + B_{12}^s\beta^2 + 2B_{66}^s\beta^2) \\ S_{22} &= A_{66}\alpha^2 + A_{22}\beta^2, \quad S_{23} = -\beta(B_{11}\beta^2 + B_{12}\alpha^2 + 2B_{66}\alpha^2), \quad S_{24} = -\beta(B_{11}^s\beta^2 + B_{12}^s\alpha^2 + 2B_{66}^s\alpha^2), \\ S_{33} &= D_{11}\alpha^4 + 2(D_{12} + 2D_{66})\alpha^2\beta^2 + D_{22}\beta^4 + K_p + K_s(\alpha^2 + \beta^2), \quad S_{34} = D_{11}^s\alpha^4 + 2(D_{12}^s + 2D_{66}^s)\alpha^2\beta^2 + D_{22}^s\beta^4, \\ S_{44} &= H_{11}^s\alpha^4 + 2(H_{12}^s + 2H_{66}^s)\alpha^2\beta^2 + H_{22}^s\beta^4 + A_{55}^s\alpha^2 + A_{44}^s\beta^2 \end{aligned} \quad (21)$$

$$\begin{aligned} m_{11} &= m_{22} = I_0, \quad m_{13} = -\alpha I_1, \quad m_{14} = -\alpha J_1, \quad m_{23} = -\beta I_1, \quad m_{24} = -\beta J_1, \quad m_{33} = I_0 + I_2(\alpha^2 + \beta^2), \\ m_{34} &= J_2(\alpha^2 + \beta^2), \quad m_{44} = K_2(\alpha^2 + \beta^2) \end{aligned} \quad (22)$$

Eq. (20) is a general form for buckling and free vibration analysis of FG plates resting on elastic foundations under in-plane loads. The stability problem can be carried out by neglecting the mass matrix while the free vibration problem is achieved by omitting the in-plane loads.

NUMERICAL EXAMPLES AND DISCUSSION

In this section various numerical examples are examined to check the accuracy of the present formulation in predicting the free vibration behaviours of simply supported FG plates resting on elastic foundation. Two types of FG plates of Al/Al₂O₃ are employed in this investigation. The material characteristics of FG plates are presented in Tab. 1. For convenience, the following non-dimensional parameters are employed:

$$\hat{\omega} = \omega b \sqrt{\rho_m / E_m}$$

Properties	Aluminium (Al)	Alumina (Al ₂ O ₃)
Young's modulus (GPa)	70	380
Poisson's ratio	0.3	0.3
Mass density kg/m ³	2702	3800

Table 1: Material properties employed in the FG plates.

In order to validate the present formulations that predict the vibration of FGM plates, various illustrative examples are presented. The present dimensionless frequency of the square FGM plate without a porosity are compared with those of



Thai and Choi [54] as shown in Tab.2. It can be observed that the results are in very good agreement with those predicted by Thai and Choi [54].

	a / b	Theory	Power law index (k)					
			0	0.5	1	2	5	10
0.5	5	Ref ⁽⁴⁹⁾	11.3952	11.2331	11.1780	11.2018	11.3593	11.4558
		Present	11.3959	11.2335	11.1783	11.2019	11.3587	11.4557
	10	Ref ⁽⁴⁹⁾	11.7257	11.4992	11.4270	11.4530	11.6243	11.7093
		Present	11.7259	11.4993	11.4271	11.4529	11.6239	11.7092
	20	Ref ⁽⁴⁹⁾	11.8246	11.5780	11.5005	11.5273	11.7054	11.7886
		Present	11.8246	11.5781	11.5005	11.5272	11.7053	11.7885
1	5	Ref ⁽⁴⁹⁾	15.3904	14.8757	14.6305	14.5004	14.5843	14.6636
		Present	15.3923	14.8768	14.6313	14.5006	14.5830	14.6635
	10	Ref ⁽⁴⁹⁾	16.1728	15.4895	15.1887	15.0455	15.1497	15.2045
		Present	16.1735	15.4898	15.1890	15.0455	15.1488	15.2043
	20	Ref ⁽⁴⁹⁾	16.4249	15.6851	15.3663	15.2209	15.3414	15.3929
		Present	16.4251	15.6852	15.3663	15.2209	15.3411	15.3928
2	5	Ref ⁽⁴⁹⁾	28.6467	26.8009	25.7640	24.9077	24.5036	24.4352
		Present	28.6591	26.8086	25.7703	24.9109	24.4983	24.4367
	10	Ref ⁽⁴⁹⁾	32.3893	29.7133	28.3322	27.2931	26.8741	26.6994
		Present	32.3937	29.7163	28.3346	27.2932	26.8675	26.6951
	20	Ref ⁽⁴⁹⁾	33.8869	30.8606	29.3467	28.2628	27.9294	27.7426
		Present	33.8882	30.8614	29.3474	28.2627	27.9267	27.7419

Table 2: Dimensionless fundamental frequency ω of rectangular plates ($k_p = k_s = 100$), $\omega = \omega \left(\frac{a^2}{b} \right) \sqrt{\rho_m / E_m}$

In order to analyse the effect of porosity on the natural frequency of FGM plates, numerical results are presented in Tabs. 2-6 and graphically plotted in Figs. 2-4.

a/h	k	$\xi=0$		$\xi=0.1$		$\xi=0.2$	
		SSDT	Present	SSDT	Present	SSDT	Present
5	0	0.4150	0.4152	0.4208	0.4210	0.4274	0.4276
	0.5	0.3550	0.3552	0.3548	0.3550	0.3544	0.3546
	1	0.3204	0.3206	0.3144	0.3146	0.3062	0.3062
	2	0.2892	0.2895	0.2754	0.2756	0.2550	0.2554
	5	0.2665	0.2674	0.2470	0.2480	0.2158	0.2170
	10	0.2554	0.2563	0.2352	0.2364	0.2026	0.2042
10	0	0.1134	0.1134	0.1149	0.1149	0.1167	0.1167
	0.5	0.0963	0.0963	0.09616	0.09616	0.09592	0.09598
	1	0.0868	0.0868	0.08498	0.08504	0.08256	0.08256
	2	0.0788	0.0788	0.07480	0.07480	0.06896	0.06896
	5	0.07398	0.07410	0.06858	0.06870	0.05978	0.05988
	10	0.07144	0.07150	0.06616	0.06628	0.05738	0.05754
20	0	0.02908	0.02908	0.02948	0.02948	0.02992	0.02992
	0.5	0.02464	0.02464	0.02460	0.02460	0.02454	0.02454
	1	0.02222	0.02222	0.02174	0.02174	0.02110	0.02110
	2	0.02018	0.02018	0.01915	0.01915	0.01762	0.01763
	5	0.01910	0.01910	0.01770	0.01771	0.01541	0.01542
	10	0.01847	0.01848	0.01715	0.01715	0.01491	0.01492

Table 3: The first non-dimensional frequencies $\hat{\omega}$ of Al/Al₂O₃ square plate for various porosity parameters, power law indices and thickness ratios (a=10h, n=m=1, K_w=K_s=0)



a/h	k	$\xi=0$		$\xi=0.1$		$\xi=0.2$	
		SSDT	Present	SSDT	Present	SSDT	Present
5	0	0.4268	0.4270	0.4336	0.4338	0.4410	0.4412
	0.5	0.3702	0.3704	0.3716	0.3716	0.3730	0.3730
	1	0.3380	0.3382	0.3342	0.3342	0.3286	0.3286
	2	0.3096	0.3098	0.2990	0.2992	0.2832	0.2834
	5	0.2900	0.2908	0.2748	0.2758	0.2508	0.2518
	10	0.2806	0.2814	0.2656	0.2664	0.2412	0.2426
10	0	0.1162	0.1162	0.1179	0.1180	0.1199	0.1200
	0.5	0.09988	0.09988	0.1001	0.1001	0.1003	0.1003
	1	0.09100	0.09100	0.08976	0.08976	0.08796	0.08802
	2	0.08362	0.08368	0.08044	0.08044	0.07578	0.07578
	5	0.07952	0.07958	0.07516	0.07528	0.06814	0.06820
	10	0.07728	0.07734	0.07318	0.07324	0.06634	0.06646
20	0	0.02976	0.02976	0.03022	0.03022	0.03074	0.03074
	0.5	0.02554	0.02554	0.02558	0.02558	0.02562	0.02564
	1	0.02326	0.02326	0.02290	0.02290	0.02244	0.02244
	2	0.02138	0.02140	0.02056	0.02056	0.01933	0.01933
	5	0.02044	0.02044	0.01932	0.01933	0.01747	0.01748
	10	0.01991	0.01991	0.01886	0.01887	0.01711	0.01712

Table 4: The first non-dimensional frequencies $\hat{\omega}$ of Al/Al₂O₃ square plate for various porosity parameters, power law indices and thickness ratios (a=10h, n=m=1, K_w=100, K_s=0).

a/h	k	$\xi=0$		$\xi=0.1$		$\xi=0.2$	
		SSDT	Present	SSDT	Present	SSDT	Present
5	0	0.4382	0.4384	0.4456	0.4458	0.4540	0.4542
	0.5	0.3844	0.3846	0.3872	0.3872	0.3900	0.3902
	1	0.3544	0.3544	0.3522	0.3524	0.3490	0.3492
	2	0.3282	0.3284	0.3204	0.3206	0.3082	0.3084
	5	0.3110	0.3118	0.2996	0.3004	0.2808	0.2814
	10	0.3032	0.3038	0.2920	0.2928	0.2736	0.2746
10	0	0.1188	0.1188	0.1208	0.1208	0.1230	0.1230
	0.5	0.1033	0.1033	0.1039	0.1039	0.1045	0.1045
	1	0.09492	0.09498	0.09412	0.09418	0.09294	0.09300
	2	0.08814	0.08814	0.08560	0.08566	0.08188	0.08194
	5	0.08448	0.08454	0.08106	0.08112	0.07536	0.07542
	10	0.08256	0.08262	0.07938	0.07952	0.07404	0.07418
20	0	0.03042	0.03042	0.03092	0.03092	0.03148	0.03148
	0.5	0.02638	0.02638	0.02652	0.02652	0.02664	0.02664
	1	0.02422	0.02422	0.02400	0.02400	0.02368	0.02368
	2	0.02250	0.02250	0.02184	0.02184	0.02084	0.02084
	5	0.02168	0.02168	0.02078	0.02078	0.01927	0.01928
	10	0.02120	0.02122	0.02040	0.02040	0.01901	0.01901

Table 5: The first non-dimensional frequencies $\hat{\omega}$ of Al/Al₂O₃ square plate for various porosity parameters, power law indices and thickness ratios (a=10h, n=m=1, K_w=0, K_s=10).

a/h	k	$\xi=0$		$\xi=0.1$		$\xi=0.2$	
		SSDT	Present	SSDT	Present	SSDT	Present
5	0	0.4494	0.4496	0.4576	0.4578	0.4668	0.4670
	0.5	0.3984	0.3986	0.4024	0.4026	0.4068	0.4068
	1	0.3702	0.3704	0.3700	0.3702	0.3688	0.3690
	2	0.3464	0.3466	0.3408	0.3410	0.3318	0.3320
	5	0.3314	0.3320	0.3230	0.3238	0.3084	0.3090
	10	0.3246	0.3252	0.3170	0.3176	0.3084	0.3042
10	0	0.1214	0.1215	0.1236	0.1237	0.1260	0.1261
	0.5	0.1067	0.1067	0.1076	0.1076	0.1085	0.1085
	1	0.09884	0.09884	0.09846	0.09846	0.09778	0.09784
	2	0.09250	0.09256	0.09064	0.09064	0.08772	0.08772
	5	0.08932	0.08940	0.08672	0.08678	0.08212	0.08218
	10	0.08766	0.08772	0.08536	0.08542	0.08120	0.08132
20	0	0.03108	0.03108	0.03164	0.03164	0.03224	0.03224
	0.5	0.02722	0.02722	0.02742	0.02742	0.02766	0.02766
	1	0.02518	0.02518	0.02508	0.02508	0.02488	0.02488
	2	0.02360	0.02360	0.02308	0.02308	0.02230	0.02230
	5	0.02288	0.02288	0.02218	0.02218	0.02096	0.02096
	10	0.02246	0.02246	0.02186	0.02186	0.02078	0.02078

Table 6: The first non-dimensional frequencies $\hat{\omega}$ of Al/Al₂O₃ square plate for various porosity parameters, power law indices and thickness ratios ($a=10h$, $n=m=1$, $K_w=100$, $K_s=10$).

Tab. 3-6 present the natural frequencies of FGM plates resting on elastic foundation for different values of porosity parameter ($\xi = 0$, $\xi = 0.1$, $\xi = 0.2$), and elastic foundation parameters. It can be seen that the results are in excellent agreement with those of Sinusoidal plate theory given by Zenkour, it is also concluded that the increase of porosity parameter leads to increase of natural frequency. It can be shown that the frequencies are increasing with the existence of (Winkler and Pasternak parameters).

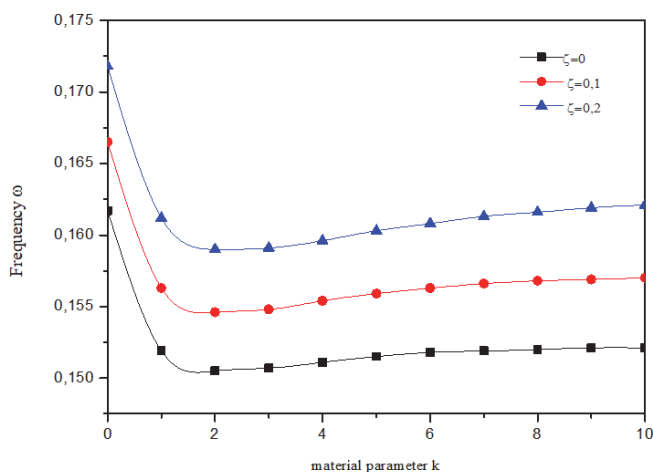


Figure 2: Variation of the natural frequency of the FGM plates according to the material power index k, mode1, $a=b$.

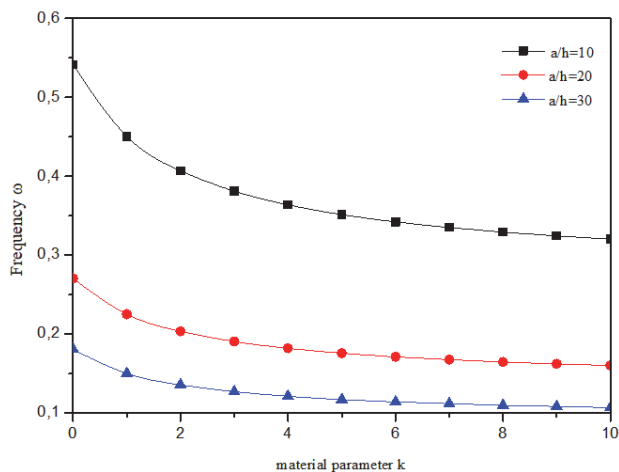


Figure 3: Influence of thickness ratio on the frequency of the plate FGM, mode 2, $\xi=0$, ($K_w = K_s = 100$).



As the material power index increases for FGM plates, the dimensionless frequency will decrease.

The variation curves of the natural frequency of the first mode of various functionally graded plates as a function of material power index parameter "k", for different values of porosity was presented in Fig. 2. It can be seen that the increase of porosity parameter leads to an increase of the frequency of the first mode.

Fig. 3 shows the influence of thickness ratio, on the natural frequency of FGM plates ($\xi=0$), the elastic foundation parameters are taken equal to ($K_w = K_s = 100$).

It can be seen that the ratio (a/h) has a considerable effect on the frequency of the FGM plate, (The later decreases with the increase of this ratio).

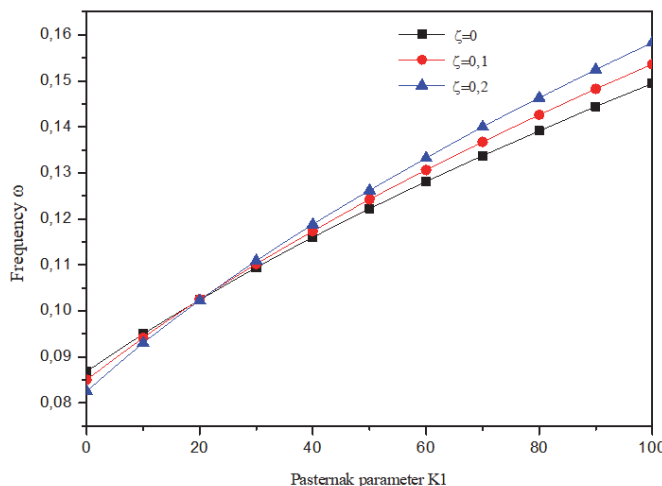


Figure 4: Effect of Pasternak shear modulus parameter on dimensionless frequency of FGM plates, $a/h=10$, $k=2$.

Fig. 4 shows the effect of Pasternak parameters on the variation of the dimensionless frequency of FGM plate for different values of porosity. The results show that the frequency increases with the increase of Pasternak parameter and porosity index.

CONCLUSION

This work proposes a new higher-order shears deformation theory for free vibration response of FG plates with porosity embedded in elastic medium. In this investigation the FGM plate are assumed to have a new distribution of porosity according to the thickness of the plate. The elastic medium is modeled as Winkler-Pasternak two parameter model to express the interaction between the FGM plate and elastic foundation. The four unknown shear deformation theory is employed to deduce the equations of motion from Hamilton's principle. The Hamilton's principle is used to derive the governing equations of motion. The accuracy of this theory is verified by compared the developed results with those obtained using others plate theory. Some examples are performed to demonstrate the effect of changing gradient material, elastic parameters, porosity index, and length to thickness ratios on the fundamental frequency of functionally graded plate.

It has been demonstrated that the present analytical formulation can accurately predict natural frequencies of FG plates with porosity resting on elastic foundation. Also it can be concluded that the effect of volume fraction distributions, slenderness ratio and porosity on the non-dimensional frequency is significant.

REFERENCES

- [1] Koizumi, M. (1997), FGM activities in Japan, Compos Part B, 28, pp. 1–4. DOI: 10.1016/S1359-8368(96)00016-9.
- [2] Akbaş, Ş. D. (2015), Wave propagation of a functionally graded beam in thermal environments, Steel and Composite Structures, 19(6), pp. 1421-1447. DOI: 10.12989/scs.2015.19.6.1421.



- [3] Bennai, R., Ait Atmane, H., Tounsi, A. (2015), A new higher-order shear and normal deformation theory for functionally graded sandwich beams, *Steel and Composite Structures*, 19(3), pp. 521 – 546. DOI: 10.12989/scs.2015.19.3.521.
- [4] Arefi, M. (2015), Elastic solution of a curved beam made of functionally graded materials with different cross sections, *Steel and Composite Structures*, 18(3), pp. 659 – 672. DOI: 10.12989/scs.2015.18.3.659.
- [5] Ait Atmane, H., Tounsi, A., Bernard, F., Mahmoud, S.R. (2015), A computational shear displacement model for vibrational analysis of functionally graded beams with porosities, *Steel and Composite Structures*, 19(2), pp. 369-384. DOI: 10.12989/scs.2015.19.2.369.
- [6] Ebrahimi, F., Dashti, S. (2015), Free vibration analysis of a rotating non-uniform functionally graded beam, *Steel and Composite Structures*, 19(5), pp. 1279 – 1298. DOI: 10.12989/scs.2015.19.5.1279.
- [7] Darilmaz, K., (2015), Vibration analysis of functionally graded material (FGM) grid systems, *Steel and Composite Structures*, 18(2), pp. 395 – 408. DOI: 10.12989/scs.2015.18.2.395.
- [8] Ebrahimi, F., Habibi, S. (2016), Deflection and vibration analysis of higher-order shear deformable compositionally graded porous plate, *Steel and Composite Structures*, 20(1), pp. 205 - 225. DOI: 10.12989/scs.2016.20.1.205.
- [9] Kar, V.R., Panda, S.K. (2016), Nonlinear thermomechanical deformation behaviour of P-FGM shallow spherical shell panel, *Chinese Journal of Aeronautics*, 29(1), pp. 173 – 183. DOI: 10.1016/j.cja.2015.12.007.
- [10] Moradi-Dastjerdi, R. (2016), Wave propagation in functionally graded composite cylinders reinforced by aggregated carbon nanotube, *Structural Engineering and Mechanics*, 57(3), pp. 441 – 456. DOI: 10.12989/sem.2016.57.3.441.
- [11] Trinh, T.H., Nguyen, D.K., Gan, B.S., Alexandrov, S. (2016), Post-buckling responses of elastoplastic FGM beams on nonlinear elastic foundation, *Structural Engineering and Mechanics*, 58(3), pp. 515 – 532. DOI: 10.12989/sem.2016.58.3.515.
- [12] Zhu, J., Lai, Z., Yin, Z., Jeon, J. and Lee, S. (2001), Fabrication of ZrO₂-NiCr functionally graded material by powder metallurgy, *Mater. Chem. Phys.*, 68(1), pp. 130-135. DOI: 10.1016/S0254-0584(00)00355-2.
- [13] Wattanasakulpong, N., Prusty, B.G., Kelly, D.W. and Hoffman, M. (2012), Free vibration analysis of layered functionally graded beams with experimental validation, *Mater. Des.*, 36, pp. 182-190. DOI: 10.1016/j.matdes.2011.10.049.
- [14] Daouadji, T.H., Adim, B., and Benferhat, B. (2018), Bending analysis of an imperfect FGM plates under hygro-thermo-mechanical loading with analytical validation, *Advances in Materials Research*, 5(1), pp. 35-53. DOI: 10.12989/amr.2016.5.1.035.
- [15] Jha, D.K., Kant, T., Singh, R.K. (2013a), A critical review of recent research on functionally graded plates, *Compos. Struct.*, 96, pp. 833–849. DOI: 10.1016/j.compstruct.2012.09.001.
- [16] Nguyen, K.T., Thai, T.H., Vo, T.P. (2015), A refined higher-order shear deformation theory for bending, vibration and buckling analysis of functionally graded sandwich plates, *Steel and Composite Structures*, 18(1), pp. 91 – 120. DOI: 10.12989/scs.2015.18.1.091.
- [17] Pradhan, K. K., Chakraverty, S. (2015), Free vibration of functionally graded thin elliptic plates with various edge supports, *Structural Engineering and Mechanics*, 53(2), pp.337 – 354. DOI: 10.12989/sem.2015.53.2.337.
- [18] Kar, V.R. and Panda, S.K. (2015), Nonlinear flexural vibration of shear deformable functionally graded spherical shell panel, *Steel Compos. Struct.*, 18(3), pp. 693-709. DOI: 10.12989/scs.2015.18.3.693.
- [19] Eltaher, M.A., Khater, M.E., Park, S., Abdel-Rahman, E., Yavuz, M. (2016), On the static stability of nonlocal nanobeams using higher-order beam theories, *Advances in Nano Research*, 4(1), pp. 51 – 64. DOI: 10.12989/anr.2016.4.1.051.
- [20] Feldman, E., Aboudi, J. (1997), Buckling analysis of functionally graded plates subjected to uniaxial loading, *Compos. Struct.*, 38, pp. 29–36. DOI: 10.1016/S0263-8223(97)00038-X.
- [21] Mahdavian, M. (2009), Buckling analysis of simply-supported functionally graded rectangular plates under non-uniform inplane compressive loading, *J. Solid Mech.*, 1, pp. 213 – 225.
- [22] Chen, C.S., Chen, T.J., Chien, R.D. (2006), Nonlinear vibration of initially stressed functionally graded plates, *Thin-Walled Struct.*, 44(8), pp. 844–851. DOI: 10.1016/j.tws.2006.08.007.
- [23] Baferani, A.H., Saidi, A.R., Jomehzadeh, E. (2011a), An exact solution for free vibration of thin functionally graded rectangular plates, *Proc. Inst. Mech. Eng. Part C*, 225, pp. 526 – 536. DOI: 10.1243/09544062JMES2171.
- [24] Praveen, G.N., Reddy, J.N. (1998), Nonlinear transient thermoelastic analysis of functionally graded ceramic-metal plates, *Int. J. Solids Struct.*, 35, pp. 4457–4476. DOI: 10.1016/S0020-7683(97)00253-9.
- [25] Croce, L.D., Venini, P. (2004), Finite elements for functionally graded Reissner–Mindlin plates. *Comput. Methods Appl. Mech. Eng.*, 193, pp. 705 – 725. DOI: 10.1016/j.cma.2003.014.



- [26] Efraim, E., Eisenberger, M. (2007), Exact vibration analysis of variable thickness thick annular isotropic and FGM plates, *J. Sound Vib.* 299, pp. 720 – 738. DOI: 10.1016/j.jsv.2006.06.068.
- [27] Zhao, X., Lee, Y.Y., Liew, K.M. (2009), Free vibration analysis of functionally graded plates using the element-free kp-Ritz method, *J. Sound Vib.* 319, pp. 918 – 939. DOI: 10.1016/j.jsv.2008.06.025.
- [28] Reddy, J.N. (2000), Analysis of functionally graded plates, *Int. J. Numer. Methods Eng.* 47, pp. 663 – 684. DOI: 10.1002/(SICI)1097-0207(20000110/30)47:1/3<663::AID-NME787>3.0.CO;2-8.
- [29] Pradyumna, S., Bandyopadhyay, J.N. (2008), Free vibration analysis of functionally graded curved panels using a higher-order finite element formulation, *J. Sound Vib.* 318, pp. 176 – 192. DOI: 10.1016/j.jsv.2008.03.056.
- [30] Jha, D.K., Kant, T., Singh, R.K. (2013b), Free vibration response of functionally graded thick plates with shear and normal deformations effects, *Compos. Struct.* 96, pp. 799 – 823. DOI: 10.1016/j.compstruct.2012.09.034.
- [31] Neves, A.M.A., Ferreira, A.J.M., Carrera, E., Cinefra, M., Roque, C.M.C., Jorge, R.M.N., Soares, C.M.M. (2013), Static, free vibration and buckling analysis of isotropic and sandwich functionally graded plates using a quasi-3D higher-order shear deformation theory and a meshless technique, *Compos. Part B*, 44, pp. 657 – 674. DOI: 10.1016/j.compositesb.2012.01.089.
- [32] Reddy, J.N. (2011), A general nonlinear third-order theory of functionally graded plates, *Int. J. Aerosp. Lightweight Struct.* 1, pp. 1–21. DOI: 10.3850/S201042861100002X.
- [33] Talha, M., Singh, B.N. (2010), Static response and free vibration analysis of FGM plates using higher order shear deformation theory, *Appl. Math. Model.* 34, pp. 3991 – 4011. DOI: 10.1016/j.apm.2010.03.034.
- [34] Chen, C., Hsu, C., Tzou, G. (2009), Vibration and stability of functionally graded plates based on a higher-order deformation theory, *J. Reinf. Plast. Compos.* 28, pp. 1215 – 1234. DOI: 10.1177/0731684408088884.
- [35] Mantari, J., Soares, C.G. (2012), Generalized hybrid quasi-3D shear deformation theory for the static analysis of advanced composite plates, *Compos. Struct.* 94(8), pp. 2561 – 2575. DOI: 10.1016/j.compstruct.2012.02.019.
- [36] Houari, M.S.A., Tounsi, A., Anwar Bég, O. (2013), Thermoelastic bending analysis of functionally graded sandwich plates using a new higher order shear and normal deformation theory, *International Journal of Mechanical Sciences*, 76, pp. 102 – 111. DOI: 10.1016/j.ijmecsci.2013.09.004.
- [37] Saidi, H., Houari, M.S.A., Tounsi, A. and Adda Bedia, E.A. (2013), Thermo-mechanical bending response with stretching effect of functionally graded sandwich plates using a novel shear deformation theory, *Steel Compos. Struct.* 15, pp. 221 – 245. DOI: 10.12989/scs.2013.15.2.221.
- [38] Matsunaga, H. (2008), Free vibration and stability of functionally graded plates according to a 2D higher-order deformation theory, *Compos. Struct.* 82, pp. 499 – 512. DOI: 10.1016/j.compstruct.2007.07.006.
- [39] Tounsi, A., Houari, M.S.A., Benyoucef, S., Adda Bedia, E.A. (2013), A refined trigonometric shear deformation theory for thermoelastic bending of functionally graded sandwich plates, *Aerospace Science and Technology*, 24, pp. 209 – 220. DOI: 10.1016/j.ast.2011.11.009.
- [40] Saidi, H., Tounsi, A., and Bousahla, A.A. (2016), A simple hyperbolic shear deformation theory for vibration analysis of thick functionally graded rectangular plates resting on elastic foundations, *Geomechanics and Engineering, An Int'l Journal*, 11 (2), pp. 289 – 307. DOI: 10.12989/gae.2016.11.2.289.
- [41] Bennai, R., Fourn, H., Ait Atmane, H., Tounsi, A. and Bessaim, A. (2018), A Dynamic and wave propagation investigation of FGM plates with porosities using a four variable plate theory, *Wind and Structures*, 28 (1), pp. 49 – 62. DOI: 10.12989/was.2019.28.1.049.
- [42] Mahi, A., Adda Bedia, E.A., Tounsi, A. (2015), A new hyperbolic shear deformation theory for bending and free vibration analysis of isotropic, functionally graded, sandwich and laminated composite plates, *Appl. Math. Modelling*, 39, pp. 2489 – 2508. DOI: 10.1016/j.apm.2014.10.045.
- [43] Bounouara, F., Benrahou, K.H., Belkorissat, I., Tounsi, A. (2016), A nonlocal zeroth-order shear deformation theory for free vibration of functionally graded nanoscale plates resting on elastic foundation, *Steel and Composite Structures*, 20(2), pp. 227 – 249. DOI: 10.12989/scs.2016.20.2.227.
- [44] Abdelbari, S., A., Fekrar, A., Heireche, H., Saidi, H., Tounsi, A., Adda Bedia, E.A. (2016), An efficient and simple shear deformation theory for free vibration of functionally graded rectangular plates on Winkler–Pasternak elastic foundations, *Wind and Structures*, 22(3), pp. 329 – 348. DOI: 10.12989/was.2016.22.3.329.
- [45] Ait Atmane, H., Tounsi, A., Bernard, F. (2016), Effect of thickness stretching and porosity on mechanical response of a functionally graded beams resting on elastic foundations, *International Journal of Mechanics and Materials in Design*, (In press). DOI: 10.1007/s10999-015-9318-x.
- [46] Chikh, A., Bakora, A., Heireche, H., Houari, M.S.A., Tounsi, A., Adda Bedia, E.A. (2016), Thermo-mechanical postbuckling of symmetric S-FGM plates resting on Pasternak elastic foundations using hyperbolic shear deformation theory, *Structural Engineering and Mechanics*, 57(4), pp. 617 – 639. DOI: 10.12989/sem.2016.57.4.617.



-
- [47] Bakora, A., Tounsi, A. (2015), Thermo-mechanical post-buckling behavior of thick functionally graded plates resting on elastic foundations, *Structural Engineering and Mechanics*, 56(1), pp.85 – 106. DOI: 10.12989/sem.2015.56.1.085.
 - [48] Tebboune, W., Benrahou, K.H., Houari, M.S.A. and Tounsi, A. (2015), Thermal buckling analysis of FG plates resting on elastic foundation based on an efficient and simple trigonometric shear deformation theory, *Steel Compos. Struct.*, 18(2), pp. 443 – 465. DOI: 10.12989/scs.2015.18.2.443.
 - [49] Meksi, A., Benyoucef, S., Houari, M.S.A., Tounsi, A. (2015), A simple shear deformation theory based on neutral surface position for functionally graded plates resting on Pasternak elastic foundations, *Structural Engineering and Mechanics*, 53(6), pp. 1215 – 1240. DOI: 10.12989/sem.2015.53.6.1215.
 - [50] Ait Amar Meziane, M., Abdelaziz, H.H., Tounsi, A. (2014), An efficient and simple refined theory for buckling and free vibration of exponentially graded sandwich plates under various boundary conditions, *Journal of Sandwich Structures and Materials*, 16(3), pp. 293 – 318. DOI: 10.1177/1099636214526852.
 - [51] Zidi, M., Tounsi, A., Houari M.S.A., Adda Bedia, E. A., Anwar Bég, O. (2014), Bending analysis of FGM plates under hygro-thermo-mechanical loading using a four variable refined plate theory, *Aerospace Sci. Technol.*, 34, pp. 24 – 34. DOI: 10.1016/j.ast.2014.02.001.
 - [52] Khalfi, Y., Houari, M.S.A. and Tounsi, A. (2014), A refined and simple shear deformation theory for thermal buckling of solar functionally graded plates on elastic foundation, *Int. J. Comput. Meth.*, 11(5), 135007. DOI: 10.1142/S0219876213500771.
 - [53] Bouderba, B., Houari, M.S.A., Tounsi, A. (2013), Thermomechanical bending response of FGM thick plates resting on Winkler–Pasternak elastic foundations, *Steel and Composite Structures*, 14(1), pp. 85 – 104. DOI: 10.12989/scs.2013.14.1.085.
 - [54] Thai, H.T., Choi, D.H. (2014), Zeroth-order shear deformation theory for functionally graded plates resting on elastic foundation, *International Journal of Mechanical Sciences*, 78, pp. 35 – 43. DOI: 10.1016/j.ijmecsci.2013.09.020.